Modeling of a Multi-Megawatt Grid Connected PV System with Integrated Batteries

Vandana Rallabandi, Oluwaseun M. Akeyo and Dan M. Ionel, *Fellow, IEEE*

SPARK Laboratory, Department of Electrical and Computer Engineering, University of Kentucky, Lexington, KY, US

vandana.rallabandi@uky.edu, m.akeyo@uky.edu, dan.ionel@uky.edu

***Abstract*—The multi-megawatt grid connected photovoltaic (PV) system studied in the paper includes parallel arrays and power electronic units, each with their own DC-DC and DC-AC converters. In one configuration, the DC-AC converters of adjacent parallel sections are connected in cascade, in order to effectively operate as a multilevel inverter, thereby reducing the filtering requirements. Grid voltage oriented control is employed for inverters and a battery is incorporated for energy storage and performance improvement. Modeling is performed with the PSCAD/EMTDC software, such that both the power electronics components, controls and subsystem aspects, and the electric grid power system issues, can be studied during steady-state and transient operation. The system simulation is demonstrated on a modified IEEE 14-bus test case.**

I. Introduction

Renewable energy generation is fast developing and solar photovoltaic (PV) systems have surpassed record installations in recent years [1]. Literature on PV related topics covers techniques for maximum power point tracking (MPPT), which were recently reviewed for example in [2], power quality improvements and specific controllers [3–5] and specific power electronic circuit topologies for DC-DC converters, DC-AC inverters, and single stage power converters [6–10]. As the irradiance inequality between PV panels connected in series may limit the power output, the focus of some of the published research is on array reconfiguration in order to balance effects [11]. Other papers propose module integrated converters, such that the MPP for each module can be tracked, yielding maximum energy extraction [12, 13]. Module integrated DC-DC converters connected to a central DC-AC converter were proposed in [14].

The current paper discusses a layout of a multi-megawatt grid connected solar PV farm with integrated battery energy storage. The PV system under study is divided into several sections, and each section has its own DC-DC converter and a two level DC-AC inverter with grid oriented voltage control as seen in Figs 1 and 2. In the proposed arrangement, the two-level inverters are cascaded in order to obtain a voltage waveform comparable with that would be available from a multi-level converter. The system and its controls are simulated on a modified IEEE 14 bus test power system using the PSCAD/EMTDC software. A battery energy storage system (BESS) is employed in order to provide power to the grid in case of partial or complete shading following a proposed control scheme according to which if the batterys state of charge is lower than the minimum allowed the adjacent synchronous generators will supply the power deficit.

II. System configuration

For high power applications, it is common to divide the PV plant into several sections as seen in in Fig. 2 [8, 15]. In each section, the PV array is connected to a buck converter, which is used to maintain the PV voltage at its maximum power point. It is reported that a buck converter has an advantage over other DC-DC converters when there are multiple strings connected in the array [14]. The output of the buck converter is connected to a central inverter, which is typically a two level inverter. The power circuit diagram of one unit is shown in Fig. 1. The battery energy storage system (BESS) is interfaced with the system such that the battery supplies power to the grid through its own inverter when there is loss of power due to shading of the PV panels.

A. Photovoltaic array

The PV cell is the component responsible for the conversion of light energy into electrical energy. A simplified equivalent circuit is used to represent the PV cell in [16]. However, this ignores the shunt resistance of the PV cell. The PV model in PSCAD/EMTDC is based on the Norton equivalent circuit with the output current(I_{cell}) given as

$$I_{cell} = I_g - I_o[e^{(\frac{V+R_{sr}}{nKT_c/q})} - 1] - (\frac{V + IR_{sr}}{R_{sh}}), \qquad (1)$$

where, I_g, is the photo current generated; I_o, the saturation current; K, the Boltzmann constant; q, the electron charge; V, the output voltage; T_c, the cell temperature; R_{sh}, the shunt resistance and R_{sr}, the series resistance.

The open circuit voltage of a PV module is dependent on the type of material used for the cell design and typically varies from 23.3 to 44.2 V when tested under standard conditions [17]. The PV module used for this array was designed to consist of 2 strings with 40 cells in series per string. This yielded an open circuit voltage of 43.7V and a short circuit current of 9.12A per module under standard test conditions (STC). The PV array used in this study consists of 160 strings of PV modules with 24 modules connected in series per string in other to restrict the DC bus voltage below 1kV.

Authors' manuscript version. The final published version is copyrighted by IEEE and available as: V. Rallabandi, O. M. Akeyo and D. M. Ionel, "Modeling of a multi-megawatt grid connected PV system with integrated batteries," *2016 IEEE International Conference on Renewable Energy Research and Applications (ICRERA)*, Birmingham, 2016, pp. 1146-1151. doi: 10.1109/ICRERA.2016.7884512.

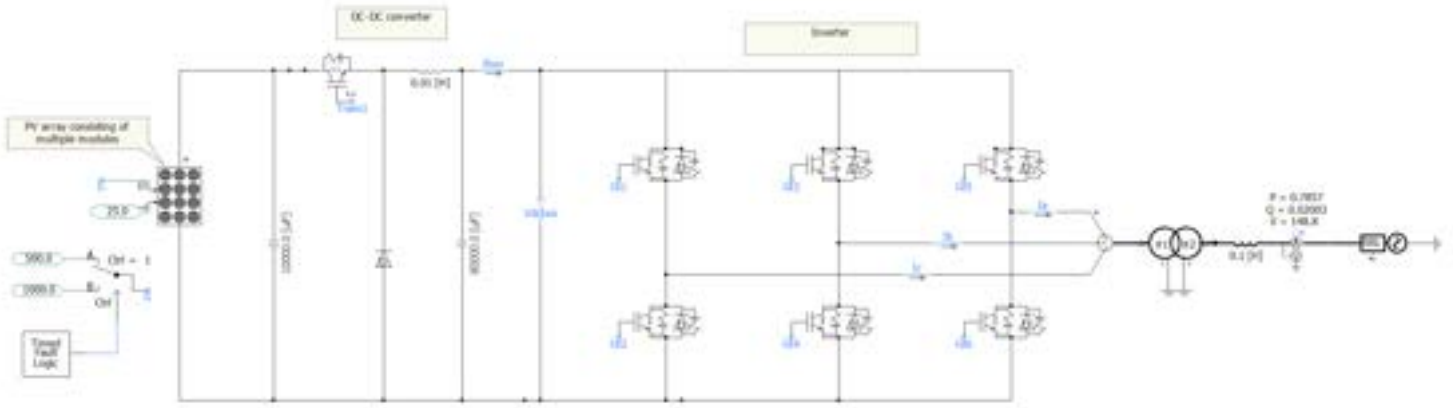

Fig. 1. Power circuit diagram in the PSCAD simulator showing a module comprising a PV array, a buck converter, a 2-level inverter, and a transformer connected to the power grid.

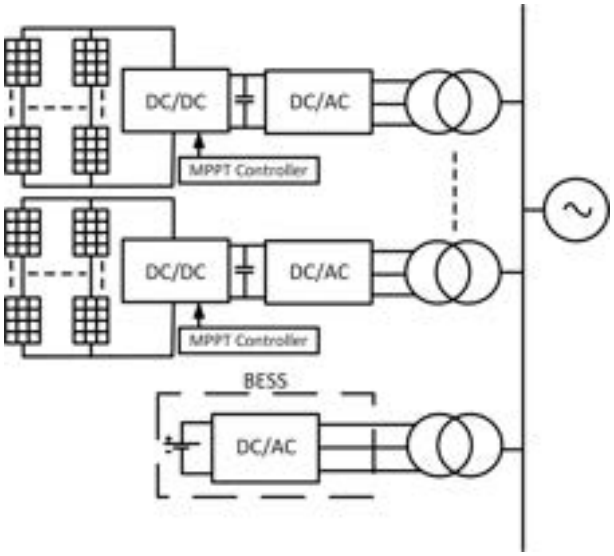

Fig. 2. Schematic of a power grid tied solar PV system consisting of several units connected in parallel. For generalization, each unit employs its own transformer, while in practice, implementations with a single / common transformer are also possible. The battery energy storage system (BEES) is connected to the power grid through its own inverter.

TABLE I
PV CELL AND MODULE SPECIFICATIONS

Parameters	Value
Cell Open circuit voltage(V)	1.09
Cell Short circuit current (A)	4.56
Module open circuit voltage(V)	43.7
Module short circuit current(A)	9.12
maximum power(W)	260

B. Maximum power point tracking

The maximum power that can be delivered by a PV array is dependent on the amount of solar irradiance and the ambient temperature of the solar cells. Since these factors are never constant and continuously changing, there is need to incorporate an algorithm to determine the maximum power point at any given atmospheric condition. Incremental Conductance and P&O methods are most widely used in MPPT. The P&O method measures the voltage and current of the PV array then perturbs the voltage by adding small disturbances and observes the change in power. If the perturbation is large, the MPP is determined faster at the expense of accuracy. Furthermore, the P&O method can fail under rapid variation of solar irradiance. The InC method of MPPT was used in this paper due to its ability to rapidly and accurately track the MPP voltage under irradiance variations [18]. The control block diagram for generating the gating pulses used for controlling the IGBT in the buck converter is shown in Fig. 3.

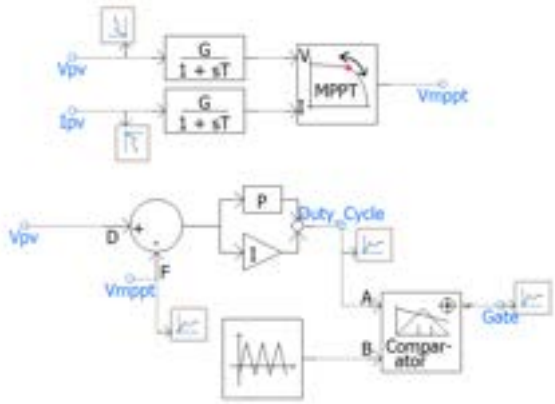

Fig. 3. Control algorithm schematic for the PV side converter employing elements from the PSCAD library.

C. Grid-connected inverter

The central 2-level inverter considered in this study has some limitations, namely large filter size to meet the required THD standards. As mentioned previously, the PV plant consists of sections with their own DC-DC and DC-AC converters connected in parallel. The requirement of large size of filter can be counteracted by the interconnection of inverter pairs

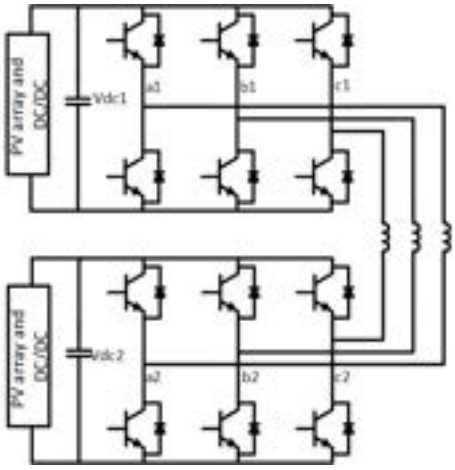

Fig. 4. Proposed connection of two 2-level inverters in other to obtain a 3 level output. The DC link voltages are maintained equal by absorbing the required amount of active power from the grid. A higher number of levels may be obtained by the interconnection of multiple inverters.

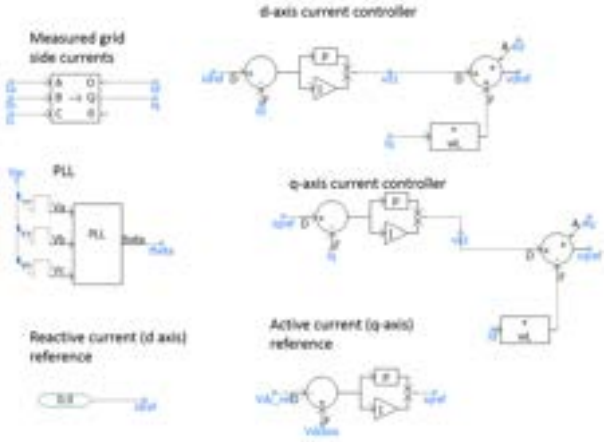

Fig. 5. Implementation of the controls for the grid side inverter using blocks from the PSCAD library. The dq components, v_d and v_q and the line reactance, ωL are decoupling terms.

in adjacent sections in cascade as shown in Fig. 4. Three - level output is obtained by maintaining the DC link voltages at the same value, and four level output can be obtained by maintaining $V_{dc2} = \frac{V_{dc1}}{2}$, while two level output is obtained when either one of the DC link voltages is 0 [19]. The DC link voltages can be maintained at the desired value by absorbing the required active power from the grid. Alternatively, the inverters in three adjacent sections may be interconnected together to obtain a 4 level output, with the predominant harmonic frequency at 3 times the switching frequency [20]. The control block diagram of the inverter is shown in Fig. 5. A grid voltage oriented control method is used for the inverter.

III. Battery energy storage system

The battery is connected to the grid through its own inverter as shown in Fig. 2. The battery is controlled in such a way that

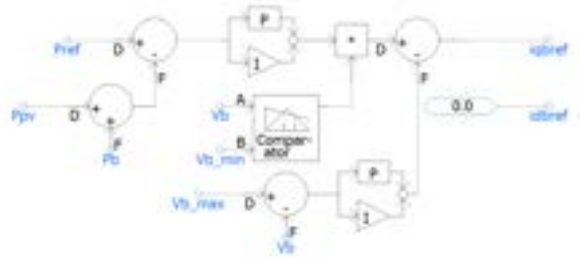

Fig. 6. Control diagram for the battery showing the voltages corresponding to maximum and minimum states of charge Vb_{max} and Vb_{min}. The d and q axes reference currents are fed to an inner current controller, or used to generate voltage references which are subsequently used to generate the gating signals (not shown).

it discharges only when the PV panel is unable to supply the required power. At other times, it charges from the grid if its state of charge is lower than the maximum [21]. The battery side inverter is also controlled by a grid voltage oriented control similar to that of the PV. The active current reference(I^*_q) is derived as the sum of the charging current component ($I^*_{q_{charge}}$) and discharging current component ($I^*_{q_{discharge}}$) as given in equation 4.

As shown in Fig. 6, the PI controller for battery discharge is used to ensure that the sum of the real power produced by the battery and PV is maintained at a specified reference value, such that the battery only supplies the amount of real power lost during shading of the PV panels. Active power is supplied by the battery as long as the terminal voltage of the battery is above the battery voltage that represents the minimum state of charge. The charging current controller outputs a current component corresponding to the amount of power required to increase the battery terminal voltage to a value that represents the maximum state of charge. The net battery current is derived as the sum of discharging and charging currents. The reactive power component I^*_d for this design was maintained at zero so that the battery does not supply reactive power, this component can also be varied.

$$I^*_{q_{discharge}} = [P_{ref} - (P_{pv} + P_{battery})] * (K_p + \frac{1}{K_i}) \quad (2)$$

when $V_b > V_{b_{minimum}}$

$$I^*_{q_{charge}} = -[V_{b_{max}} - V_{battery})] * (K_p + \frac{1}{K_i}), \quad (3)$$

when $V_b < V_{b_{minimum}}$

$$I^*_q = I^*_{q_{discharge}} + I^*_{q_{charge}} \quad (4)$$

IV. Simulation Results

One unit of a grid connected PV array was simulated using PSCAD/EMTDC software. Simulation results of Figs. 8, 9, 10, 11 and 12 show the effect of a step change in insolation at t = 10s. on the system in Fig. 1. The action of the BESS, following shading of the PV panels is shown in Fig. 14.

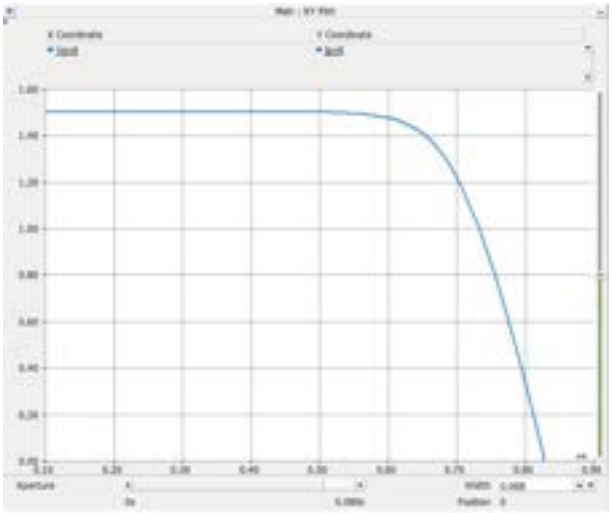

Fig. 7. The I-V characteristic of a PV cell for $1000W/m^2$ insolation with V and A units on the x and y axis, respectively. The output power of the PV cell has a non-linear variation with a maximum reached at the knee of the curve.

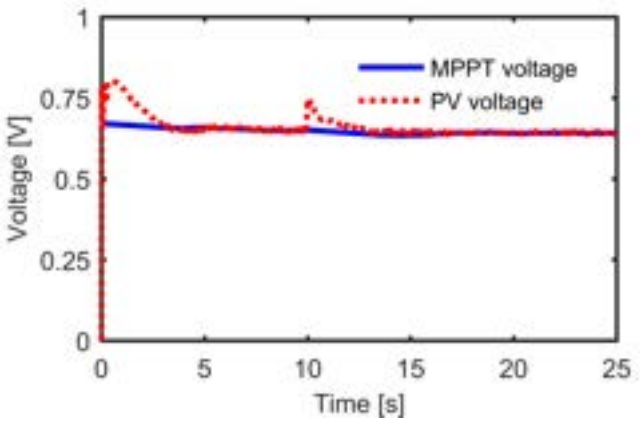

Fig. 8. Results for simulation of the system from Fig. 1 considering a step change in insolation at t = 10s. The PV output voltage follows the MPPT voltage irrespective of change in insolation.

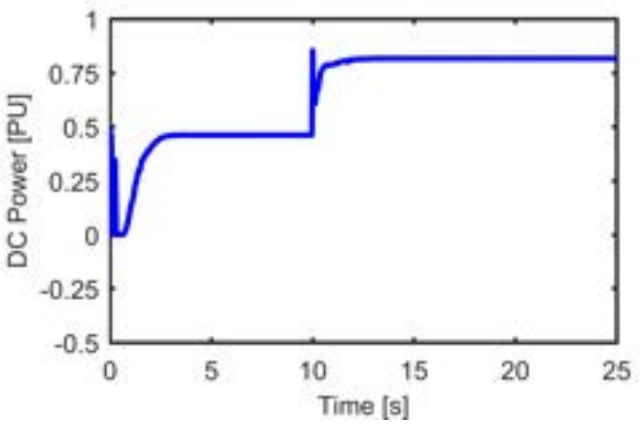

Fig. 9. The DC power from the PV panels increases following the change in insolation from 500W/m^2 to 1000W/m^2 at t = 10s.

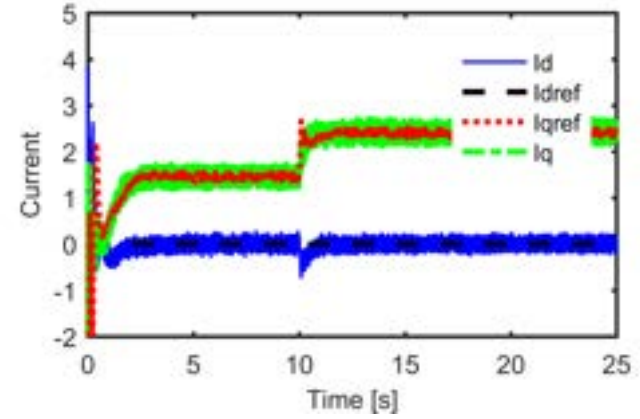

Fig. 10. The reactive, d-axis, and active, q-axis, currents are maintained at their respective references following the change in insolation. In this example, the d-axis current is maintained at zero value, and the q-axis current is determined by the power input.

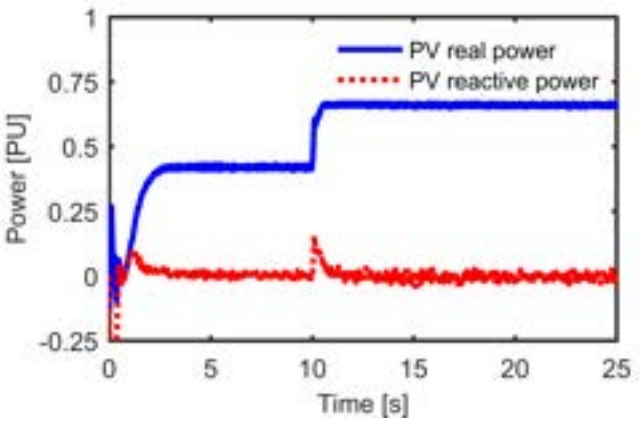

Fig. 11. Variations of active and reactive power. In this example, zero reactive power is delivered to the grid during steady-state operation, and the active power follows the change in insolation.

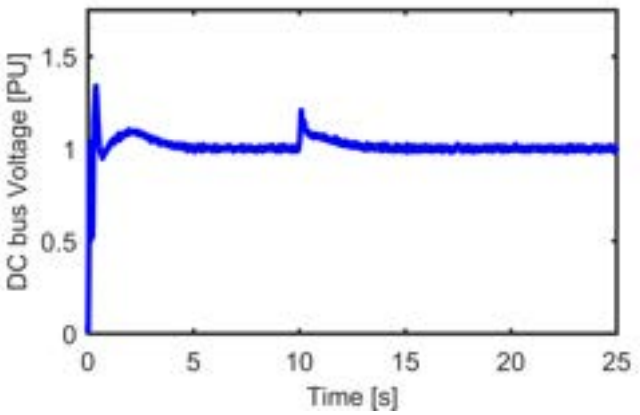

Fig. 12. The control loop maintains the DC link voltage constant at 560 V by regulating the q-axis current irrespective of the insolation.

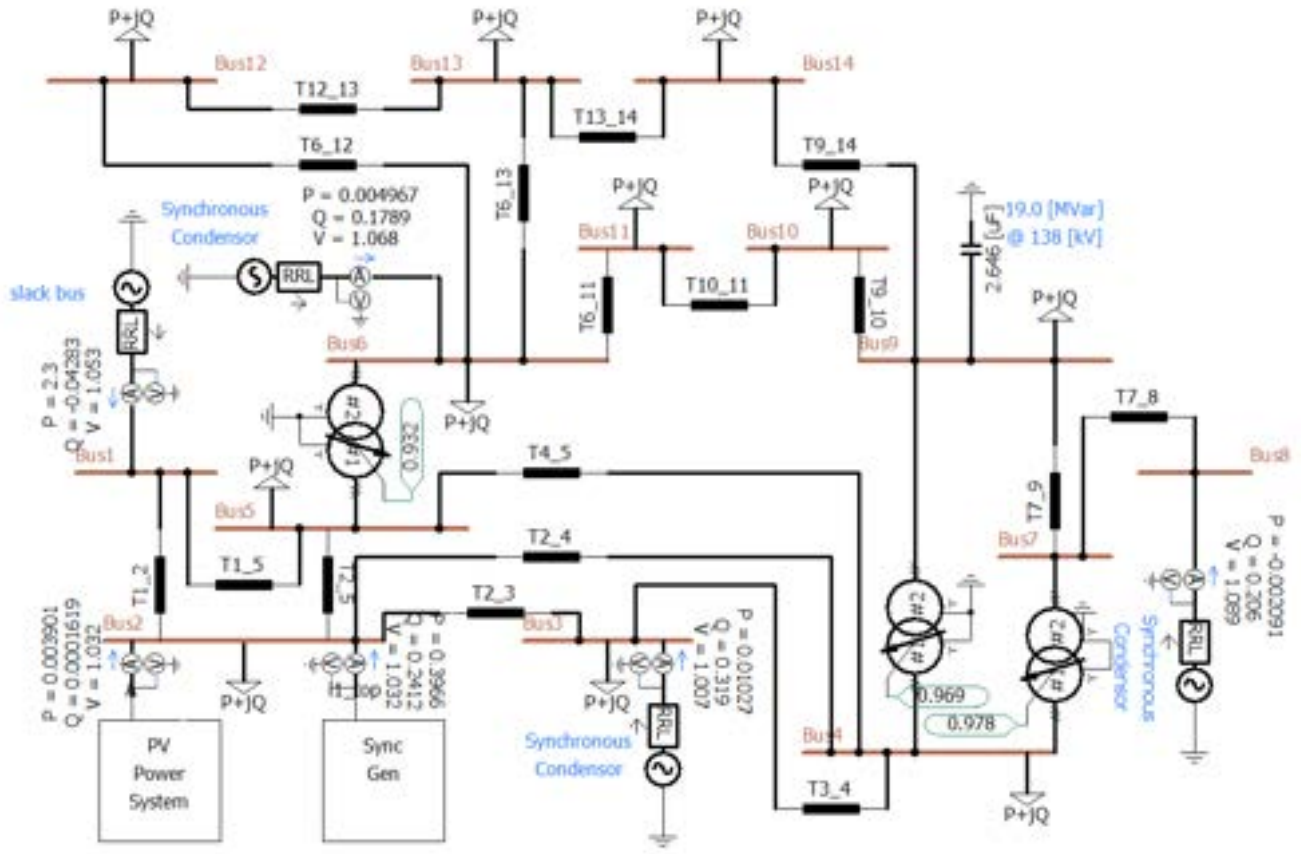

Fig. 13. Circuit diagram for the modified IEEE 14 Bus system considered in the study. The PV farm is connected to the second bus.

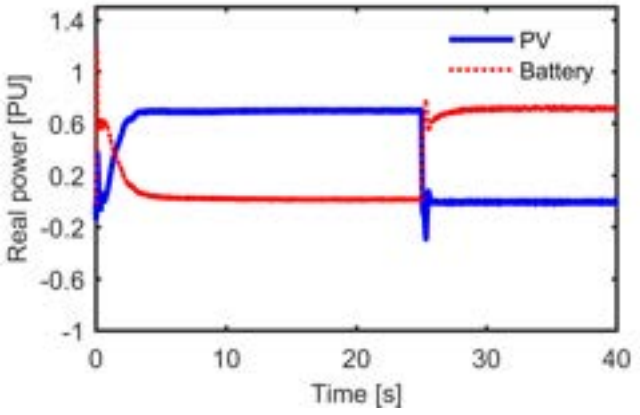

Fig. 14. Simulation results for system in Fig. 1, with a BESS. At time t = 25s, the PV array is completely shaded and the battery compensates for the power deficit without supplying any reactive power to the grid.

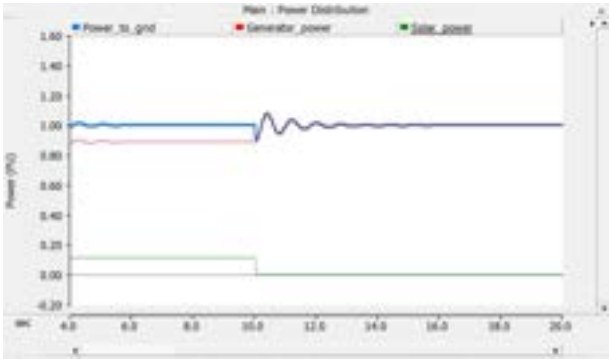

Fig. 15. Simulation results for a total loss of power from the PV panel at t = 10s. Before this event, power is supplied by both the PV system and the synchronous generator coupled on the same bus. After the event, the synchronous generator supplies the power deficit, provided that the battery is unavailable due to a low state of charge.

The IEEE 14-bus system is a transmission network widely used for short circuit analysis, load flow studies, and grid interconnection problems. The PV system supplies part of the power at Bus no. 2 as shown in Fig. 13 [22]. In the case considered here, the PV power rating is only a fraction of the rating of the total rating of the generation at Bus no. 2. In case of complete shading of the PV array, and if the battery has a state of charge below minimum, the synchronous generator at Bus no. 2 will step up its output power to supply the connected loads as shown in Fig. 15. In case of higher PV penetration, the power deficit resulting from shading would be divided among different generators for optimum economic dispatch. Further,

the PV converter can be controlled to supply reactive power at night, while absorbing a small amount of active power to maintain the DC link voltage.

V. Conclusion

The multi-MW PV system studied in paper has a modular topology and includes a proposed parallel connection of two-level inverters in order to generate a multi-level type output. As a result, in conjunction with a grid voltage oriented control for the active and reactive power components, the quality of the output waveforms is improved and the filtering requirements are reduced. A battery energy storage system (BESS) is incorporated and a control algorithm is proposed in order to minimize the negative transient effects due to PV panel shading. The benefits of the system are demonstrated through simulation using the PSCAD/EMTDC software, such that both the power electronics and power systems aspects are considered in detail. The study included the simulation of a modified IEEE 14-bus system, incorporating a PV system and an adjacent synchronous generator.

Acknowledgment

Special thanks are due to Dr. Om Nayak and his team at Nayak Corp. for expert advice on the PSCAD simulation software. The support of University of Kentucky, the L. Stanley Pigman endowment, and the Power and Energy Institute of Kentucky (PEIK) are gratefully acknowledged.

References

[1] F. Blaabjerg and D. M. Ionel, "Renewable energy devices and systems state-of-the-art technology, research and development, challenges and future trends," *Electric Power Components and Systems*, vol. 43, no. 12, pp. 1319–1328, 2015.

[2] E. Koutroulis and F. Blaabjerg, "Overview of maximum power point tracking techniques for photovoltaic energy production systems," *Electric Power Components and Systems*, vol. 43, no. 12, pp. 1329–1351, 2015.

[3] T. Noguchi, S. Togashi, and R. Nakamoto, "Short-current pulse-based maximum-power-point tracking method for multiple photovoltaic-and-converter module system," *IEEE Transactions on Industrial Electronics*, vol. 49, no. 1, pp. 217–223, Feb 2002.

[4] T. L. Kottas, Y. S. Boutalis, and A. D. Karlis, "New maximum power point tracker for pv arrays using fuzzy controller in close cooperation with fuzzy cognitive networks," *IEEE Transactions on Energy Conversion*, vol. 21, no. 3, pp. 793–803, Sept 2006.

[5] A. Kalbat, "Pscad simulation of grid-tied photovoltaic systems and total harmonic distortion analysis," in *Electric Power and Energy Conversion Systems (EPECS), 2013 3rd International Conference on*, Oct 2013, pp. 1–6.

[6] V. Vekhande and B. G. Fernandes, "Module integrated dc-dc converter for integration of photovoltaic source with dc microgrid," in *IECON 2012 - 38th Annual Conference on IEEE Industrial Electronics Society*, Oct 2012, pp. 5657–5662.

[7] B. M. T. Ho, S. H. Chung, and S. Y. R. Hui, "An integrated inverter with maximum power tracking for grid-connected pv systems," in *Applied Power Electronics Conference and Exposition, 2004. APEC '04. Nineteenth Annual IEEE*, vol. 3, 2004, pp. 1559–1565 Vol.3.

[8] S. Essakiappan, H. S. Krishnamoorthy, P. Enjeti, R. S. Balog, and S. Ahmed, "Multilevel medium-frequency link inverter for utility scale photovoltaic integration," *IEEE Transactions on Power Electronics*, vol. 30, no. 7, pp. 3674–3684, July 2015.

[9] S. Jain and V. Agarwal, "A single-stage grid connected inverter topology for solar pv systems with maximum power point tracking," *IEEE Transactions on Power Electronics*, vol. 22, no. 5, pp. 1928–1940, Sept 2007.

[10] V. Vekhande, N. Kothari, and B. G. Fernandes, "Switching state vector selection strategies for paralleled multilevel current-fed inverter under unequal dc-link currents condition," *IEEE Transactions on Power Electronics*, vol. 30, no. 4, pp. 1998–2009, April 2015.

[11] G. Velasco-Quesada, F. Guinjoan-Gispert, R. Pique-Lopez, M. Roman-Lumbreras, and A. Conesa-Roca, "Electrical pv array reconfiguration strategy for energy extraction improvement in grid-connected pv systems," *IEEE Transactions on Industrial Electronics*, vol. 56, no. 11, pp. 4319–4331, Nov 2009.

[12] Y. Zhou, L. Liu, and H. Li, "A high-performance photovoltaic module-integrated converter (mic) based on cascaded quasi-z-source inverters (qzsi) using egan fets," *IEEE Transactions on Power Electronics*, vol. 28, no. 6, pp. 2727–2738, June 2013.

[13] C. T. Pan, M. C. Cheng, C. M. Lai, and P. Y. Chen, "Current-ripple-free module integrated converter with more precise maximum power tracking control for pv energy harvesting," *IEEE Transactions on Industry Applications*, vol. 51, no. 1, pp. 271–278, Jan 2015.

[14] G. R. Walker and P. C. Sernia, "Cascaded dc-dc converter connection of photovoltaic modules," *IEEE Transactions on Power Electronics*, vol. 19, no. 4, pp. 1130–1139, July 2004.

[15] Y. Yang and F. Blaabjerg, "Overview of single-phase grid-connected photovoltaic systems," *Electric Power Components and Systems*, vol. 43, no. 12, pp. 1352–1363, 2015.

[16] S.-K. Kim, J.-H. Jeon, C.-H. Cho, E.-S. Kim, and J.-B. Ahn, "Modeling and simulation of a grid-connected {PV} generation system for electromagnetic transient analysis," *Solar Energy*, vol. 83, no. 5, pp. 664 – 678, 2009.

[17] I. H. Mahammed, Y. Bakelli, S. H. Oudjana, A. H. Arab, and S. Berrah, "Optimal model selection for pv module modeling," in *2012 24th International Conference on Microelectronics (ICM)*, Dec 2012, pp. 1–4.

[18] D. P. Hohm and M. E. Ropp, "Comparative study of maximum power point tracking algorithms using an experimental, programmable, maximum power point tracking test bed," in *Photovoltaic Specialists Conference, 2000. Conference Record of the Twenty-Eighth IEEE*, 2000, pp. 1699–1702.

[19] K. A. Corzine, S. D. Sudhoff, and C. A. Whitcomb, "Performance characteristics of a cascaded two-level converter," *IEEE Transactions on Energy Conversion*, vol. 14, no. 3, pp. 433–439, Sep 1999.

[20] E. Cengelci, S. U. Sulistijo, B. O. Woo, P. Enjeti, R. Teoderescu, and F. Blaabjerg, "A new medium-voltage pwm inverter topology for adjustable-speed drives," *IEEE Transactions on Industry Applications*, vol. 35, no. 3, pp. 628–637, May 1999.

[21] K. Sun, L. Zhang, Y. Xing, and J. M. Guerrero, "A distributed control strategy based on dc bus signaling for modular photovoltaic generation systems with battery energy storage," *IEEE Transactions on Power Electronics*, vol. 26, no. 10, pp. 3032–3045, Oct 2011.

[22] "Ieee 14 bus knowledge base," https://hvdc.ca/knowledge-base/read,article/26/ieee-14-bus-system/v:, accessed: 2016-08-03.